Magnetic moment of ¹⁰⁴Agᵐ and the hyperfine magnetic field of Ag in Fe using nuclear magnetic resonance on oriented nuclei

V. V. Golovko,[1,*] I. S. Kraev,[1] T. Phalet,[1] B. Delauré,[1] M. Beck,[1] V. Yu. Kozlov,[1] S. Coeck,[1] F. Wauters,[1] P. Herzog,[2]
Ch. Tramm,[2] D. Zákoucký,[3] D. Vénos,[3] D. Srnka,[3] M. Honusek,[3] U. Köster,[4,5] and N. Severijns[1]

[1]*Instituut voor Kern-en Stralingsfysica, Katholieke Universiteit Leuven, Celestijnenlaan 200D, B-3001 Leuven, Belgium*
[2]*Helmholtz-Institut für Strahlen- und Kernphysik, Universität Bonn, D-53115 Bonn, Germany*
[3]*Nuclear Physics Institute, ASCR, CZ-250 68 Řež, Czech Republic*
[4]*Institut Laue Langevin, 6 rue Jules Horowitz, F-38042 Grenoble Cedex 9, France*
[5]*ISOLDE, CERN, CH-1211 Genève 23, Switzerland*

Nuclear magnetic resonance (NMR/ON) measurements with β- and γ-ray detection have been performed on oriented ¹⁰⁴Ag^{g,m} nuclei with the NICOLE ³He-⁴He dilution refrigerator setup at ISOLDE/CERN. For ¹⁰⁴Ag^g ($I^\pi = 5^+$) the γ-NMR/ON resonance signal was found at $\nu = 266.70(5)$ MHz. Combining this result with the known magnetic moment for this isotope, the magnetic hyperfine field of Ag impurities in an Fe host at low temperature (<1 K) is found to be $|B_{\rm hf}({\rm Ag}Fe)| = 44.709(35)$ T. A detailed analysis of other relevant data available in the literature yields three more values for this hyperfine field. Averaging all four values yields a new and precise value for the hyperfine field of Ag in Fe; that is, $|B_{\rm hf}({\rm Ag}Fe)| = 44.692(30)$ T. For ¹⁰⁴Ag^m ($I^\pi = 2^+$), the anisotropy of the β particles provided the NMR/ON resonance signal at $\nu = 627.7(4)$ MHz. Using the new value for the hyperfine field of Ag in Fe, this frequency corresponds to the magnetic moment $\mu(^{104m}{\rm Ag}) = +3.691(3)$ $\mu_{\rm N}$, which is significantly more precise than previous results. The magnetic moments of the even-A ¹⁰²⁻¹¹⁰Ag isotopes are discussed in view of the competition between the $(\pi g_{9/2})^{-3}_{7/2^+}(\nu d_{5/2}\nu g_{7/2})_{5/2^+}$ and the $(\pi g_{9/2})^{-3}_{9/2^+}(\nu d_{5/2}\nu g_{7/2})_{5/2^+}$ configurations. The magnetic moments of the ground and isomeric states of ¹⁰⁴Ag can be explained by an almost complete mixing of these two configurations.

I. INTRODUCTION

Nuclear magnetic moments are an important tool for the study of nuclear structure because they provide a sensitive test of the nuclear coupling scheme. The light even-A ¹⁰²⁻¹¹⁰Ag isotopes provide a very interesting case. In the heavier ¹⁰⁶⁻¹¹⁰Ag isotopes the $(\pi g_{9/2})^{-3}_{7/2^+}$ proton group and the $(\nu d_{5/2})^{-1}_{5/2^+}$ neutron state couple to produce $I^\pi = 1^+$ and $I^\pi = 6^+$ ground and isomeric states, respectively. In the lighter ¹⁰²⁻¹⁰⁴Ag isotopes the ground and isomeric states have, respectively, $I^\pi = 5^+$ and $I^\pi = 2^+$ and result from a mixture of the $(\pi g_{9/2})^{-3}_{7/2^+}$ and $(\pi g_{9/2})^{-3}_{9/2^+}$ proton groups coupling to a $(\nu d_{5/2}\nu g_{7/2})^n_{5/2^+}$ neutron configuration, where $n = 5$ or 7. (Henceforth, for brevity, the neutron occupation n will be omitted.) Thus, whereas in most cases isomeric states have excitation energies of several hundred keV and a higher spin than the corresponding ground state, the silver isotopes ¹⁰²,¹⁰⁴Ag provide a different picture: The excitation energies of the isomeric states do not exceed a few keV, and their spins are lower than those of the ground states. The exact nature of the mixing of different configurations to produce the wave functions of these isomeric and ground states turns out to be an intriguing problem, to which precise values of

the nuclear magnetic moments of these states can provide important information.

The nucleus ¹⁰⁴Ag has a $I^\pi = 5^+$ ground state with half-life $t_{1/2} = 69$ min and a $I^\pi = 2^+$ isomeric state with $t_{1/2} = 33.5$ min at an excitation energy of only 6.9 keV. For the $I^\pi = 5^+$ ground state the magnetic moment was determined with high accuracy in a γ-NMR/ON measurement as $\mu = 3.914(8)$ $\mu_{\rm N}$ [1] and later also in an atomic beam magnetic resonance experiment; that is, $\mu = 3.919(3)$ $\mu_{\rm N}$ [2]. For the isomeric state, the only value for the magnetic moment that is available in the literature, that is, $\mu = +3.7(2)$ $\mu_{\rm N}$ [3], is not very precise though. Note that by careful comparison of the works of Ames *et al.* [3], Greenebaum and Phillips [4], and van Walle [5], we found that the value $\mu = 4.12(25)$ $\mu_{\rm N}$ listed for ¹⁰⁴Ag^m in Table 3.8 of Ref. [5], which was copied in Ref. [6] and later also in Ref. [7], is in fact the value that was obtained by Greenebaum and Phillips [4] for ¹⁰²Ag^m.

Previously, the proton ground-state configuration of ¹⁰⁴Ag was found to be a mixture of the $(\pi g_{9/2})^{-3}_{7/2^+}$ and $(\pi g_{9/2})^{-3}_{9/2^+}$ proton groups [3]. A clear indication for a transition from $(\pi g_{9/2})^{-3}_{7/2^+}$ being the dominant component in the wave function to $(\pi g_{9/2})^{-3}_{9/2^+}$ was found when going from ¹⁰³Ag (with $I^\pi = 7/2^+$) to ¹⁰¹Ag (with $I^\pi = 9/2^+$) and also when going from ¹⁰⁶Ag to ¹⁰²Ag [5]. For the isomeric state ¹⁰⁴Ag^m with $I^\pi = 2^+$, a mixing of these two proton groups was assumed on the basis of the not very precise magnetic moment value from an atomic beam experiment [3]. We have therefore performed a new measurement on ¹⁰⁴Ag^m to get a more precise value for the magnetic moment of this isomeric state, thus

_____

*vgolovko@owl.phy.queensu.ca; present address: Department of Physics, Queen's University, Stirling Hall, Kingston, Ontario K7L3N6, Canada.

making it possible to shed more light on its exact configuration, as well as on the evolution of the proton configuration in the $^{102-106}$Ag isotopes. The method of nuclear magnetic resonance on oriented nuclei was used, observing the destruction of the β-particle emission asymmetry by radio frequency radiation (β-NMR/ON). The nuclei were oriented with the method of low-temperature nuclear orientation [8].

^{104}Ag^m was obtained from the decay of ^{104}Cd parent nuclei ($t_{1/2} = 57.7$ min) that were implanted in the sample foil. As the ^{104}Ag ground state was found to be present in the sample as well, we measured in the same experimental run also the resonance signal for ^{104g}Ag. The fact that the magnetic moment of this state had previously been determined already with good accuracy from hyperfine structure measurements, yielding $\mu = 3.913(3) \, \mu_N$ [2], allowed us to obtain a new and precise value for the hyperfine field of Ag impurities in Fe.

Note, finally, that the magnetic moment of ^{104m}Ag determined here also served as calibration for a measurement of the β-emission asymmetry in the decay of this isotope for the study of isospin mixing [9].

II. EXPERIMENTAL DETAILS

A. Sample preparation and detection setup

The Ag isotopes used for the NMR/ON studies reported here were obtained from the decay of the ^{104}Cd precursor produced at the ISOLDE facility [10,11]. The radioactive ^{104}Cd ($t_{1/2} = 57.7$ min) was produced with a 1.4-GeV proton beam (8×10^{12} protons per pulse, staggered mode) from the CERN Proton Synchrotron Booster accelerator (PS Booster), bombarding a tin liquid-metal target [12]. Reaction products diffused out of the target and effused via a hot transfer line to the ion source. The atoms were ionized to 1^+ ions, extracted, accelerated to 60 keV, and then mass separated by the ISOLDE General Purpose Separator (GPS). Finally, the ^{104}Cd beam was transported through the beam distribution system and implanted into a 125-μm-thick, 99.99% pure iron foil soldered onto the cold finger of the ^{3}He-^{4}He refrigerator of the NICOLE low-temperature nuclear orientation setup [13,14]. The iron foil supplied by Goodfellows was first polished and then annealed under a hydrogen atmosphere at $\approx 800°$C for about 6 h.

Prior to the implantation of the ^{104}Cd beam, a polarizing magnetic field of $B_{ext} = 0.5$ T was applied with the superconducting split-coil magnet in the refrigerator to fully magnetize the iron foil. This field was then lowered to $B_{ext} = 0.1008(3)$ T to reduce its influence on the trajectories of the β particles. The fact that part (i.e., about 10% [15]) of the saturation magnetization of the Fe foil was lost when the field was reduced to this lower value slightly reduced the sensitivity but did not further affect the measurements.

The geometry of the experimental setup was very similar to the one we used for our previous β-NMR/ON experiments [9,17,18] and is shown schematically in Fig. 1. The angular distribution of β particles was observed with two planar HPGe particle detectors [19,20] with a sensitive area of about 110 mm^2 mounted inside the 4 K radiation shield of the refrigerator at a distance of about 32 mm from the
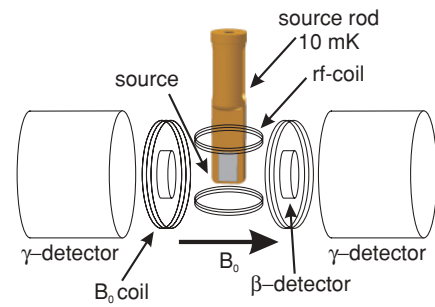

FIG. 1. (Color online) Schematic layout of the experimental setup. The radioactive sample is prepared by implanting the ISOLDE beam, which is not shown here and is arriving perpendicular to the plane of the drawing, in the Fe foil on the Cu sample holder. A polarizing magnetic field B_{ext} is created by the split-coil superconducting magnet. The RF coil provides a field perpendicular to B_{ext} for the NMR/ON measurements. The β particles are observed with planar HPGe detectors installed inside the 4 K shield of the refrigerator at an angle of about 15° with respect to the magnetic field B_{ext}. Large-volume HPGe γ detectors are installed outside the refrigerator.

sample. Operating these detectors inside the 4 K radiation shield, i.e., without any material between source and detector, avoids energy losses and reduces scattering of the β particles. They were mounted at an angle of 15° with respect to the magnetization axis (viz. the horizontal external magnetic field axis) to minimize the influence of scattering effects in the Fe host foil. Thin isolated copper wires (about 13 cm long) connected the detectors to the preamplifiers that were placed outside the refrigerator, resulting in an energy resolution of about 3 keV for 1-MeV β particles.

Angular distributions of γ rays were observed with three large-volume HPGe detectors with an energy resolution of about 3 keV at 1332 keV. These were placed outside the refrigerator, two along the magnetization axis (see Fig. 1) and one perpendicular to it. They served to observe the γ rays of the Ag isotopes, as well as to monitor the temperature of the sample by observing the anisotropy of the 136-keV γ ray from a calibrated ^{57}CoFe nuclear orientation thermometer [21,22] that was soldered on the back side of the sample holder.

B. Angular distribution formalism

The angular distribution of radiation emitted from an axially symmetric ensemble of oriented nuclei is given by [23]

$$W(\theta) = 1 + f \sum_{\lambda} B_{\lambda}(\mu B_{tot}/k_B T, I) U_{\lambda} A_{\lambda} Q_{\lambda} P_{\lambda}(\cos\theta), \tag{1}$$

where f represents the fraction of the nuclei that experience the full orienting hyperfine interaction, while the rest $(1 - f)$ is supposed to feel no orienting interaction at all; the B_{λ} describe the nuclear orientation; the U_{λ} are the deorientation coefficients which account for the effect of unobserved intermediate radiations; the A_{λ} are the directional distribution coefficients which depend on the properties of the observed radiation and the nuclear levels involved; the Q_{λ} are solid

angle correction factors; and $P_\lambda(\cos\theta)$ are the Legendre polynomials. The detection angle θ is measured relative to the direction of the saturation magnetization axis of the Fe host foil which is defined by the applied horizontal magnetic field. The orientation coefficients B_λ depend on the temperature of the sample T, the spin I, the magnetic moment μ of the oriented state, and the total magnetic field B_{tot} the nuclei experience (with k_B the Boltzmann constant). This field is given by

$$B_{\mathrm{tot}} = B_{\mathrm{hf}} + B_{\mathrm{ext}}(1 + K) - B_{\mathrm{dem}}, \qquad (2)$$

where B_{hf} is the hyperfine magnetic field of Ag in Fe (see Sec. IV A), B_{ext} is the externally applied field, K is the Knight shift parameter, and B_{dem} is the demagnetization field [24].

Three measurements of the Knight shift for silver in iron are reported in the literature. All three determined the Knight shift in γ-NMR/ON experiments, yielding $K(^{106}\mathrm{Ag}Fe) = -0.03(2)$ [25], $K(^{107g}\mathrm{Ag}Fe) = -0.08(8)$ [26], and $K(^{110m}\mathrm{Ag}Fe) = -0.047(5)$ [27]. We will use here the weighted average of these three results; that is, $K(\mathrm{Ag}Fe) = -0.046(5)$.

For γ rays only λ-even terms occur in Eq. (1). For positrons from allowed β decays, only the $\lambda = 1$ term is present and Eq. (1) transforms to [23]

$$W(\theta) = 1 + f\frac{v}{c}B_1 A_1 Q_1 \cos\theta, \qquad (3)$$

where v/c is the positron velocity relative to the speed of light.

Experimentally, the angular distribution is obtained by

$$W(\theta) = \frac{N_{\mathrm{cold}}(\theta)}{N_{\mathrm{warm}}(\theta)}, \qquad (4)$$

with $N_{\mathrm{cold,warm}}(\theta)$ the count rates when the sample is "cold" (about 10 mK; oriented nuclei) or "warm" (about 1 K; unoriented nuclei). In on-line experiments, where the count rates vary with beam intensity, it is customary to construct a double ratio, combining count rates in two different detectors to eliminate effects of beam intensity fluctuations and avoid the need to correct for the lifetime of the isotope. In the present work the double ratio

$$R = \left[\frac{N(15^\circ)}{N(165^\circ)}\right]_{\mathrm{cold}} \bigg/ \left[\frac{N(15^\circ)}{N(165^\circ)}\right]_{\mathrm{warm}} \qquad (5)$$

was used for the β particles and

$$R = \left[\frac{N(0^\circ)}{N(90^\circ)}\right]_{\mathrm{cold}} \bigg/ \left[\frac{N(0^\circ)}{N(90^\circ)}\right]_{\mathrm{warm}} \qquad (6)$$

was used for γ rays. All data were corrected for the dead time of the data-acquisition system using a precision pulse generator.

C. NMR/ON resonance setup and formalism

For the NMR/ON measurements a RF oscillating field was applied perpendicular to the external magnetic field (see Fig. 1). The NMR coil producing this oscillating field consisted of a pair of two-turn coils mounted on a Teflon frame that was fixed inside the 300-mK radiation shield surrounding the sample. The coil was fed from the top of the refrigerator

by coaxial cables connected to a digital Marconi frequency generator with a range from 10 kHz to 3.3 GHz. In addition to the NMR coil, a pickup coil for monitoring the RF signal was present. A linear RF amplifier with a constant gain of 46 dBm was installed between the frequency generator and the RF coil. The intensity of the RF signal was kept as small as possible to avoid too-strong RF heating and subsequent reduction in anisotropy for the β particles and γ rays.

The resonance measurements were performed at sample temperatures in the range from 8 to 12 mK by scanning the radio frequency, ν, and observing the variation of the anisotropy of the β particles and γ rays emitted by the Ag nuclei. At resonance, transitions between the Zeeman split nuclear sublevels are induced that partially equalize the originally unequal populations of the sublevels, thus reducing the degree of nuclear orientation and therefore the magnitude of the anisotropy $R - 1$. The resonance frequency ν_{res} is related to the nuclear magnetic moment through the relation

$$\nu_{\mathrm{res}}[\mathrm{MHz}] = \left|\frac{7.6226\mu[\mu_{\mathrm{N}}]B_{\mathrm{tot}}[\mathrm{T}]}{I[\hbar]}\right|. \qquad (7)$$

When promille precision is required and the nucleus is situated in a medium other than vacuum and being subject to an external applied magnetic field, the nuclear magnetic moment value has to be corrected for diamagnetism. This is a reduction of the field experienced by the nuclei owing to the polarization of the medium, which leads to an apparent reduction in the nuclear magnetic dipole moment if no correction to the applied field strength is made. The corrected magnetic moment value is then given by

$$\mu_{\mathrm{corr}} = \mu_{\mathrm{uncorr}}\left[1 - \sigma\frac{B_{\mathrm{ext}}}{B_{\mathrm{ext}} + B_{\mathrm{hf}}}\right]^{-1}, \qquad (8)$$

with σ the diamagnetic correction. For silver nuclei $\sigma = 0.005555$ [6].

III. DATA COLLECTION AND ANALYSIS

Owing to the rather long half-life of both isotopes and their rather large magnetic hyperfine interaction strengths $T_{\mathrm{int}} = |\mu B/k_{\mathrm{B}}I|$, that is, $T_{\mathrm{int}} \simeq 13$ mK for $^{104}\mathrm{Ag}^g$ and $T_{\mathrm{int}} \simeq 30$ mK for $^{104}\mathrm{Ag}^g$, relaxation of the nuclear spins to thermal equilibrium was sufficiently fast and no problems with incomplete spin-lattice relaxation [28–30] were expected.

The decay of the 5^+ $^{104}\mathrm{Ag}^g$ ground state (Fig. 2) is distributed over many EC/β^+ branches, resulting in three rather intense γ rays with energies of 555.8, 767.6, and 941.6 keV and intensities of 93%, 66%, and 25%, respectively. Whereas the 555.8-keV transition is also clearly present in the decay of the isomeric state, the β decay of the isomer contributes very little (i.e., only $\simeq 1\%$) to the intensity of the 767.6-keV transition, while the 941.6-keV transition is even completely absent in the decay of the isomer [16]. The last two γ rays are therefore especially well suited for the determination of the magnetic moment of $^{104}\mathrm{Ag}^g$ in a γ-NMR/ON experiment.

For $^{104}\mathrm{Ag}^m$ the main EC/β^+ branch represents $\simeq 70\%$ of the total decay strength and populates the 2^+ level at 555.8 keV
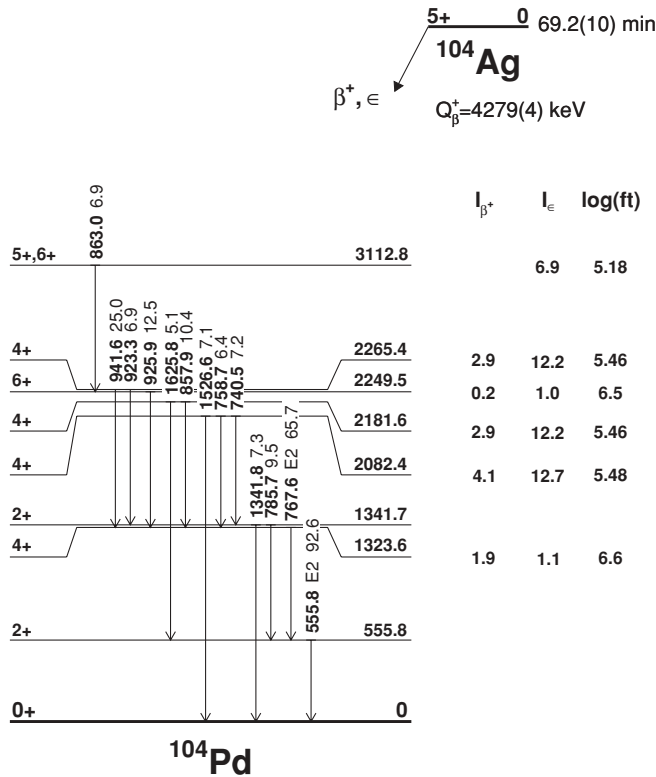
FIG. 2. Partial decay scheme of ^{104}Ag^g showing only those γ transitions with intensities larger than 5% and the related levels and EC/β decay branches. The most intense γ lines, with energies of 555.8, 767.6, and 941.6 keV, were used for the γ-NMR/ON measurements.

in ^{104}Pd [16]. All other branches represent less than 2% each of the total decay strength. Because the 555.8-keV γ transition depopulating the 2^+ first excited state is also one of the stronger γ lines in the decay of ^{104}Ag^g (see Fig. 2) and the next most intense γ transition in the decay of ^{104}Ag^m has an intensity of only about 4%, it was decided to use the β transition to the first excited state to search for the resonance signal of ^{104m}Ag.

Typical γ-ray and β-particle spectra are shown in Figs. 3 and 4, respectively.

A. γ-NMR/ON on ^{104g}AgFe

The nuclear magnetic resonance signal for the ground-state ^{104}Ag^g was obtained by observing the change of the anisotropy of the 555.8-, 767.6-, 941.6-keV γ rays as a function of the frequency of the applied RF field. Using a triangular modulation frequency of 100 Hz, a modulation bandwith of 0.5 MHz, and a RF signal level of -32 dBm, the center RF frequency was varied in steps of 0.5 MHz over the resonance search region from 263.5 to 270 MHz. The search region could be chosen so narrow because two precise and mutually consistent values are available in the literature for both the hyperfine field of Ag in Fe, that is, $|B_{hf}(\text{Ag}Fe)| = 44.7$ T [25,34], and the magnetic moment of ^{104}Ag^g, that is, $\mu = 3.92\ \mu_N$ [1,2]. Two scans were performed, stepping the frequency region in both upward and downward directions, to
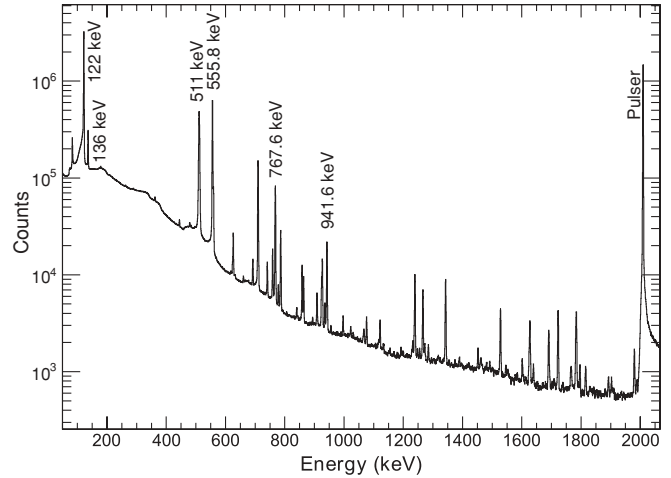

FIG. 3. Typical γ spectrum for ^{104}Ag^{g,m}, obtained in 300 s of counting. The 511-keV positron annihilation line, the 122- and 136-keV γ lines of the ^{57}CoFe nuclear thermometer, and the 555.8-, 767.6-, 941.6-keV γ-ray lines that were used for the γ-NMR/ON measurements on ^{104g}Ag are indicated. Most γ lines belong to the decay of ^{104g,m}Ag (see Ref. [16]). The strong line between the 555.8- and 767.6-keV lines is the 709-keV internal transition in ^{104}Cd.

avoid possible shifts of the (effective) resonance centers owing to a finite spin-lattice relaxation time. At each frequency, data were accumulated for 300 s.

An NMR effect was observed for all three γ rays (see, e.g., Fig. 5). Table I summarizes the results of the fits of a Gaussian line and a linear background to the data for the three different lines with the MINUIT minimization package [32]. The weighted average of the three central frequencies, obtained in a magnetic field of $B_{ext} = 0.1008(3)$ T, is

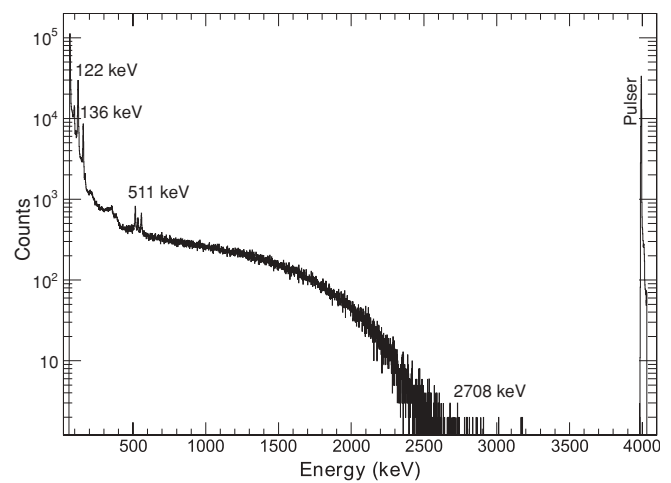$$|\nu_{res}(^{104}\text{Ag}^m Fe)| = 266.70(5) \text{ MHz.} \qquad (9)$$

FIG. 4. Typical β spectrum for ^{104}Ag^m, obtained in 300 s of counting. The end-point energy for the decay of ^{104}Ag^m (i.e., 2708 keV) is indicated. At low energy, the 122- and 136-keV γ rays from the ^{57}CoFe nuclear thermometer, the 511-keV annihilation peak, and the 555.8-keV γ ray from the ^{104}Ag^{g,m} decays are also visible.
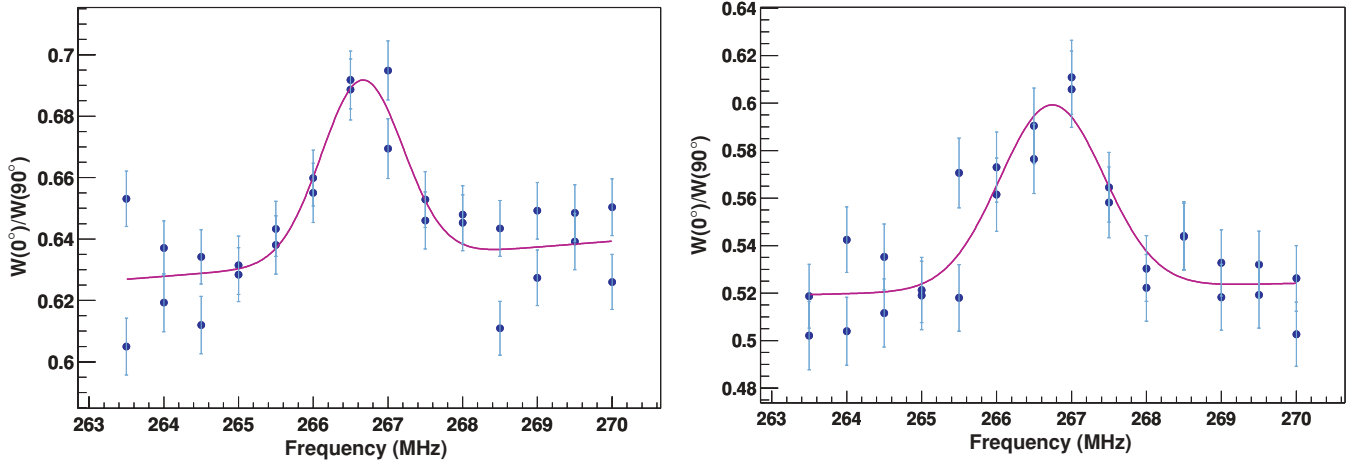
FIG. 5. (Color online) Online γ-NMR/ON curves for the 767.6-keV (a) and the 941.6-keV (b) γ lines of ^{104}Ag^g. The ratio of the pulser-normalized γ anisotropies $W(0°)/W(90°)$ is plotted as a function of RF frequency. Data points for two scans (one in upward and one in downward direction) are superposed. The integrated destruction of γ anisotropy is about 25% in both cases. The corresponding resonance frequencies are given in Table I.

This value is in agreement with, but an order of magnitude more precise than the previous result obtained in a similar experiment by Vandeplassche *et al.* [1]; that is, $\nu_{res} = 266.3(5)$ MHz. It was used to determine a new precision value for the hyperfine field of Ag in Fe, as is discussed below.

B. β-NMR/ON on ^{104}Ag^{m}Fe

To determine the magnetic moment of the isomeric state, the change of the β-particle anisotropy as a function of the RF frequency was observed. The only value for the magnetic moment of ^{104}Ag^m available in the literature is not very precise; that is, $\mu(^{104}$Ag$^m) = +3.7(2)$ μ_N [3]. The magnetic moment was therefore first determined, prior to our measurement but during the same beam time, by scanning the frequency of the first of the two lasers used to selectively ionize Ag atoms in the RILIS ion source [33]. Online analysis of this laser scan yielded

$$\mu(^{104}\mathrm{Ag}^m) = 3.7(1)\ \mu_N, \tag{10}$$

corresponding to a frequency $\nu_{res} = 630 \pm 17$ MHz, which was then used as the search region for the β-NMR/ON experiment.

To maximize statistics, the destruction of the β anisotropy effect,

$$R = 1 - \frac{W(15°)}{W(165°)}, \tag{11}$$

TABLE I. γ-NMR/ON resonance center frequencies (ν_{res}) obtained for the three most intense γ rays in the decay of ^{104}Ag^g.

Energy (keV)	ν_{res} (MHz)
555.8	266.77(13)
767.6	266.66(6)
941.6	266.74(9)
Weighted average	266.70(5)

was monitored in the energy region from 600 keV to the end point at 2708 keV. In spite of the fact that the magnitude of a β anisotropy decreases toward lower energies because of its dependence on v/c [see Eq. (3)], the size of the anisotropy was still rather large; that is, $R \simeq 0.50$. The energy region below 600 keV was not used because it suffered from background of Compton-scattered 511-keV annihilation and 555.8-keV decay γ rays. A triangular modulation frequency of 100 Hz was again used. Several frequency scans were performed. For most of these the frequency step width was 2 MHz and the modulation amplitude ± 1 MHz with a nominal RF power level of -42 dBm. For each scan the frequency region was always stepped in both upward and downward directions. No difference between the center frequencies was found for passes in opposite directions, indicating that relaxation effects were indeed negligible.

The first scans were performed with continuous modulation of the RF signal. These data were again fitted using a simple Gaussian with a constant background. Thereafter, four scans were performed by recording the spectrum for each frequency first without and immediately thereafter with frequency modulation. This FM-off/FM-on mode was used to obtain a better definition of the line shape. This was considered to be helpful because resonance lines in iron hosts at high frequencies are rather broad owing to the inhomogeneous broadening of about 1%. Figure 6 shows the destruction, S, of the β asymmetry as a function of frequency. This destruction S is defined as the difference between the ratio $W(15°)/W(165°)$ with FM on and FM off normalized to the ratio with FM off:

$$S = \frac{\left(\left[\frac{W(15°)}{W(165°)}\right]_{FMon} - \left[\frac{W(15°)}{W(165°)}\right]_{FMoff}\right)}{\left[\frac{W(15°)}{W(165°)}\right]_{FMoff}}. \tag{12}$$

The total destruction observed was about 4%. This value is smaller than in our previous experiments with ^{59}Cu ($S \approx 45\%$) [17] and ^{69}As ($S \approx 10\%$) [18] and also smaller than the destruction obtained here for the ^{104}Ag^g resonances
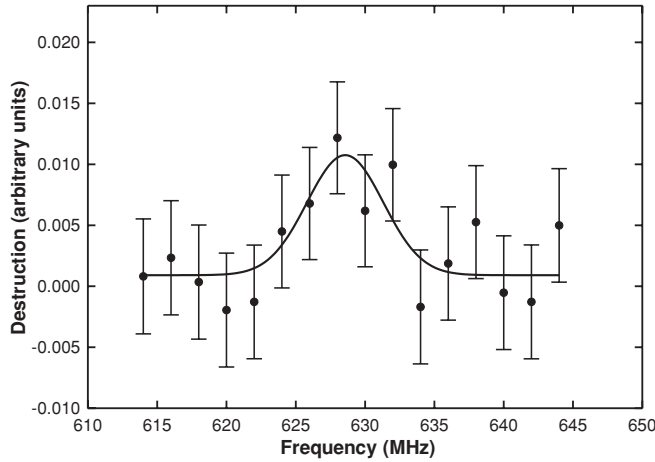
FIG. 6. β-NMR/ON resonance curve for ^{104}Ag$^m Fe$. Data from three frequency scans using the FM-off/FM-on sequence have been summed. The destruction of anisotropy is defined in Eq. (12). The total destruction observed was about 4%.

(i.e., $S \approx 25\%$) (Fig. 5). This is most probably due to the nonresonant background from β particles of the nonresonant ^{104g}AgFe in the energy region used for analysis. Nevertheless, the resonance frequency value could still be determined with good accuracy. Table II lists the results for the various scans that were performed. The weighted average resonance frequency, again obtained in a magnetic field of $B_{ext} = 0.1008(3)$ T, is

$$\nu_{res}(^{104}\text{Ag}^m Fe) = 627.7(4) \text{ MHz.} \tag{13}$$

IV. RESULTS

A. Hyperfine field of Ag impurities in Fe

To extract a precise magnetic moment value for ^{104}Ag^m from the NMR/ON frequency obtained, a precise value for the hyperfine magnetic field of Ag impurities in Fe

TABLE II. β-NMR/ON results for various scans of ^{104m}Ag. Every measurement consists of two scans over the frequency region from 613 to 647 MHz, one in upward and the other in downward direction. The measurements were performed with different step sizes and for different measurement times. The weighted average of the seven individual measurements (i.e., 14 scans) is indicated as well.

Measurement	Modulation	ν_{res} (MHz)	Step (MHz)	Collection time (s)
1	On	628.3(8)	2	150
2	On	627.0(8)	2	300
3	On	628.3(9)	5	300
4	Off/On	627.2(7)	2	300
5	Off/On	628.0(11)	2	150
6	Off/On	629.1(29)	2	150
7	Off/On	628.1(19)	2	150
$\bar{\nu}_{res}$		627.7(4)		

host, $B_{hf}(\text{Ag}Fe)$, is required. Two values are quoted in the literature. The first, $|B_{hf}(\text{Ag}Fe)| = 44.72(2)$ T, was obtained in a NMR/ON experiment with ^{110}Ag^m in Fe [34]. However, from the reported resonance frequency of 203.75(10) MHz in a field of 0.220 T, and with the magnetic moment of 3.604(4) μ_N used by the authors, one obtains $|B_{hf}(\text{Ag}Fe)| = 44.72(5)$ T, that is, the same value but with a significantly larger error bar. It seems that the error on the magnetic moment was neglected in Ref. [34]. Later, Eder *et al.* [25] quoted the value $|B_{hf}(\text{Ag}Fe)| = 44.69(5)$ T which they deduced from the NMR/ON frequency $\nu(^{110}\text{Ag}^m Fe) = 204.78(2)$ MHz reported in Ref. [35] and the magnetic moment value $|\mu(^{110}\text{Ag}^m)| = 3.607(4) \mu_N$ from Refs. [36] and [37]. In the mean time, several new hyperfine interaction measurements on ^{110}Ag^m, ^{106}Ag^m, and ^{104}Ag^g have been reported, allowing one to deduce four precise values for $B_{hf}(\text{Ag}Fe)$, as is discussed in the following paragraphs. An overview is given in Table III.

Two values for $B_{hf}(\text{Ag}Fe)$ can be obtained from data for ^{110}Ag^m. The two magnetic moment values for ^{110}Ag^m reported in Refs. [38] and [39] agree well and, after being corrected for diamagnetism [6], lead to the weighted average value $|\mu(^{110}\text{Ag}^m)| = 3.608(3) \mu_N$. Combining this with the resonance frequency for this isotope in Fe host reported in Ref. [35], that is, $\nu(^{110}\text{Ag}^m Fe) = 204.78(2)$ MHz, Eq. (7) yields for the hyperfine field of Ag impurities in Fe the value

$$|B_{hf}(\text{Ag}Fe)|_1 = 44.675(37) \text{ T.} \tag{14}$$

Note that no correction for the Knight shift is required as the resonance frequency was quoted for $B_{ext} = 0$, while a correction for B_{dem} can be neglected at the present level of precision because a very thin foil was used.

Further, the nuclear magnetic moment of ^{110}Ag^m cited above, that is, $|\mu(^{110}\text{Ag}^m)| = 3.608(3) \mu_N$, and the resonance frequency $|\nu(^{110m}\text{Ag}Fe)| = 203.75(10)$ MHz reported in Ref. [34] yield $|B_{tot}(\text{Ag}Fe)| = 44.451(43)$ T. The frequency was obtained with a 3-μm-thick foil, rendering the correction for B_{dem} again negligible, and in $B_{ext} = 0.220$ T. Taking then also the Knight shift parameter $K = -0.046(5)$ into account (which was not yet known at the time of Ref. [34]), one derives from Eq. (2)

$$|B_{hf}(\text{Ag}Fe)|_2 = 44.661(43) \text{ T.} \tag{15}$$

A third value for $|B_{hf}(\text{Ag}Fe)|$ is obtained from data for ^{106m}Ag: NMR/ON resonance frequencies for this isotope were determined in both a Ag and an Fe host. Eder *et al.* [26], obtained $|\nu(^{106}\text{Ag}^m Fe)| = 210.57(3)$ MHz in $B_{ext} = 0$ with a stack of foils of 2 μm thickness (such that $B_{dem} = 0$). Ohya *et al.* [40] reported $|\nu(^{106}\text{Ag}^m Ag)| = 56.128(26)$ MHz in an external field of about 12 T. The exact value of this applied field could be deduced from the resonance frequency of ^{110}Ag^m in Ag for the same field setting, which was found at 54.640(1) MHz [41].

Using for the magnetic moment of ^{110m}Ag the weighted average value from Refs. [38] and [39], that is, $|\mu(^{110}\text{Ag}^m)_{uncorr}| = 3.588(3) \mu_N$ (this time not corrected for diamagnetism because the nuclear orientation in the NMR/ON experiments of Refs. [40] and [41] was induced solely by an external magnetic field), Eq. (7) yields $|B_{tot}| = 11.987(10)$ T.

TABLE III. Input data leading to the hyperfine magnetic field for Ag impurities in Fe and the values obtained from these.

Line	Measured/deduced quantity	Value	Ref.	Remark
1	$\|\mu(^{110}\text{Ag}^m)\|$	3.607(4) μ_{N}[a]	[38]	ABMR[b]
2	$\|\mu(^{110}\text{Ag}^m)\|$	3.609(4) μ_{N}[a]	[39]	BF-NMR/ON[c]
3	$\|\mu(^{110}\text{Ag}^m)\|$	3.608(3) μ_{N}		Weighted average of above two values
4	$\|\nu(^{110}\text{Ag}^m Fe)\|$	204.78(2) MHz	[35]	NMR/ON, for $B_{\text{ext}} = 0$ T
5	$\|B_{\text{hf}}(\text{Ag}Fe)\|$	44.675(37) T		From the resonance frequency in line 4 and the magnetic moment value in line 3
6	$\|\nu(^{110}\text{Ag}^m Fe)\|$	203.75(10) MHz	[34]	NMR/ON, in $B_{\text{ext}} = 0.220$ T
7	$\|B_{\text{hf}}(\text{Ag}Fe)\|$	44.661(43) T		From the resonance frequency in line 6 and the magnetic moment value in line 3
8	$\|\nu(^{106}\text{Ag}^m Fe)\|$	210.57(3) MHz	[26]	NMR/ON, for $B_{\text{ext}} = 0$ T
9	$\|\nu(^{106}\text{Ag}^m Ag)\|$	56.128(26) MHz	[40]	BF-NMR/ON[c] in $B_{\text{tot}} = 11.987$ T
10	$\|B_{\text{hf}}(\text{Ag}Fe)\|$	44.720(43) T		From the ratio of the resonance frequencies in lines 8 and 9 [see also Eq. (16)]
11	$\|\nu(^{104}\text{Ag}^g Fe)\|$	266.70(5) MHz	This work	NMR/ON, in $B_{\text{ext}} = 0.1008$ T
12	$\|\mu(^{104}\text{Ag}^g)\|$	3.919(3) μ_{N}	[2]	Optical spectroscopy
13	$\|B_{\text{hf}}(\text{Ag}Fe)\|$	44.709(35) T		From the resonance frequency of this work (line 11) and the magnetic moment value in line 12
14	$\|B_{\text{hf}}(\text{Ag}Fe)\|$	44.692(30) T		Weighted average of the values in lines 5, 7, 10, and 13

[a]Corrected for diamagnetism according to [6].

[b]Atomic beam magnetic resonance.

[c]Brute-force nuclear magnetic resonance on oriented nuclei.

The ratio $r = 3.7516(18)$ of the two aforementioned frequencies for ^{106}Ag^m can be written as

$$r = \frac{\mu(^{106}\text{Ag}^m)_{\text{corr}}|B_{\text{hf}}(\text{Ag}Fe)|}{\mu(^{106}\text{Ag}^m)_{\text{uncorr}}|B_{\text{tot}}|}$$

$$= \frac{1.005586|B_{\text{hf}}(\text{Ag}Fe)|}{11.987(10)\text{T}}, \qquad (16)$$

with $\mu(^{106}\text{Ag}^m)_{\text{corr}}/\mu(^{106}\text{Ag}^m)_{\text{uncorr}} = 1.005\,586$ the factor for the diamagnetic correction [6], so that

$$|B_{\text{hf}}(\text{Ag}Fe)|_3 = 44.720(43) \text{ T}. \qquad (17)$$

Finally, a hyperfine field value can also be obtained from data for ^{104}Ag^g. Indeed, combining our NMR/ON resonance frequency for ^{104}Ag^g in Fe, that is, $|\nu(^{104}\text{Ag}^m Fe)| = 266.70(5)$ MHz, with the magnetic moment value $|\mu(^{104}\text{Ag}^m)| = 3.919(3)$ μ_{N} from optical hyperfine spectroscopy measurements [2], Eq. (7) yields $|B_{\text{tot}}(\text{Ag}Fe)| = 44.639(35)$ T. Correcting this result according to Eq. (2) for the external magnetic field $B_{\text{ext}} = 0.1008(3)$ T, for the Knight shift parameter $K = -0.046(5)$, and for the demagnetization of the 125-μm-thick Fe foil used, that is, $B_{\text{dem}} = 0.026(5)$ T (a 20% error was adopted to account for approximations made in the equations used to calculate B_{dem} [9]), results in

$$|B_{\text{hf}}(\text{Ag}Fe)|_4 = 44.709(35) \text{ T}. \qquad (18)$$

When combining the four aforementioned hyperfine fields to one weighted average, the correlations between the first three values, which all rely on the same value for the magnetic moment of ^{110m}Ag, were duly taken into account by incorporating the full covariance matrix (e.g., [46]). Using then further standard error propagation techniques yields for

the magnetic hyperfine field of Ag impurities in Fe the value

$$|B_{\text{hf}}(\text{Ag}Fe)| = 44.692(30) \text{ T} \qquad (19)$$

(the error would be 0.020 T instead of 0.030 T if correlations would not have been taken into account). This value is in agreement with and more precise than the value of 44.69(5) T cited in Ref. [25]. It will be used further in the analysis of our NMR/ON results for ^{104}Ag^m in the next section.

B. Nuclear magnetic moment of ^{104m}Ag

With the value for the hyperfine magnetic field of Ag impurities in Fe being established, we can now deduce a precise value for the magnetic moment of ^{104}Ag^m from our resonance frequency $|\nu(^{104}\text{Ag}^m Fe)| = 627.7(4)$ MHz. Taking into account the external field $B_{\text{ext}} = 0.1008(3)$ T and the Knight shift parameter $K = -0.046(5)$, and correcting for the demagnetization field opposite to the direction of the external field, that is, $B_{\text{dem}} = 0.026(5)$ T (see earlier in this article), the total magnetic field experienced by the nuclei is found to be $|B_{\text{tot}}| = 44.622(30)$ T. Equation (7) then yields for the magnetic moment

$$|\mu(^{104}\text{Ag}^m)| = 3.691(3) \ \mu_{\text{N}}. \qquad (20)$$

Correcting for diamagnetism does not change this value. This is the first precision value for the magnetic moment of this isomer.

V. MAGNETIC MOMENTS OF $^{102-110}$Ag

The magnetic moments of the odd-odd even-A Ag isotopes are listed in Table IV.

TABLE IV. Experimental magnetic-moment values for the ground and isomeric states of the even-A isotopes $^{102-110}$Ag. Whenever a diamagnetic correction was applied, this is indicated. In all other cases, the correction was either negligibly small or not necessary because of the method that was applied or because of the large experimental error bar.

Isotope	I	μ (μ_N)	Ref.
^{102}Ag^g	5	4.55(65)	[42][a]
^{104}Ag^g	5	3.916(8)[b]	[1,5][c]
		3.919(3)	[2][d]
		+4.0(2)	[3][e]
^{106}Ag^g	1	+2.83(20)	[4][e]
^{108}Ag^g	1	2.6884(7)[f]	[43][c]
^{110}Ag^g	1	2.7271(8)[f]	[43][c]
^{102}Ag^m	2	+4.12(25)	[4][e]
^{104}Ag^m	2	3.691(3)	This work[c]
		3.7(1)	This work[g]
		+3.7(2)	[3][e]
^{106}Ag^m	6	3.705(4)	[40][h]
		3.709(4)	[25][c]
		3.71(15)	[44][a]
		3.82(8)	[45][a]
^{108}Ag^m	6	3.577(20)	[36][d]
^{110}Ag^m	6	3.607(4)[b,f]	[38][e]
		3.609(4)[b,f]	[39][h]

[a]Low-temperature nuclear orientation.
[b]Recalculated using the hyperfine field value obtained in the previous section.
[c]Nuclear magnetic resonance on oriented nuclei.
[d]Optical hyperfine spectroscopy.
[e]Atomic beam magnetic resonance.
[f]Corrected for diamagnetism.
[g]Resonant laser ionization source technique.
[h]Brute-force nuclear magnetic resonance on oriented nuclei.

Extended magnetic-moment calculations for even-A odd-odd Ag isotopes are not available in the literature. Table V presents an overview of the experimental values for the magnetic moments of the ground and isomeric states in the even-A $^{102-110}$Ag isotopes, as well as a comparison with values calculated with the additivity rule [49],

$$\mu_I[\mu_N] = \frac{1}{2}I(g_n + g_p)$$
$$+ \frac{(g_n - g_p)[I_n(I_n + 1) - I_p(I_p + 1)]}{2(I + 1)}. \quad (21)$$

For this we used Schmidt single-particle moments and modified single-particle moments, as well as the mean values of experimental magnetic moments of neighboring odd-even nuclei.

The Schmidt single-particle magnetic moments for the $\pi g_{9/2}$ and $\nu d_{5/2}$ orbitals that determine the spins and magnetic moments of the light $^{101-110}$Ag nuclei are +6.793 μ_N and −1.913 μ_N, respectively [50]. Modified single-particle moments take into account the effects of the nuclear medium, that is, configuration mixing, core polarization, and meson exchange [51], by using the effective gyromagnetic ratios

$g_l^{mod}(\pi) = +1.1$, $g_l^{mod}(\nu) = -0.05$, and $g_s^{mod} = 0.7\, g_s^{free}$, that is, $g_s^{mod}(\pi) = 3.910$ and $g_s^{mod}(\nu) = -2.678$, thus yielding $\mu^{mod}[\pi(g_{9/2})] = +6.355\,\mu_N$ and $\mu^{mod}[\nu(d_{5/2})] = -1.439\,\mu_N$. Finally, using experimental g factors from neighboring odd-even nuclei has the advantage that configuration mixing and possible g-factor quenching in the odd-A nuclei are automatically taken into account. For the g factor of the $g_{9/2}$ protons, the value of the lower-mass odd-A silver isotope was used each time. For the g factor of the $d_{5/2}$ neutrons, the geometrical mean of the g factors of the neighboring isotopes of Ru, Pd, and Cd with the neutron in the $d_{5/2}$ orbital were used.

Note that nearly all neighboring odd-neutron Ru, Pd, Cd, and Sn isotopes with $N = 55, 57, 59, 61$, and 63 have a $5/2^+$ ground state. For the isotopes with $N = 55$, this is attributable to the hole in the $\nu d_{5/2}$ orbit. For the isotopes with $N = 57$ to 63, filling the $\nu g_{7/2}$ orbit, this indicates that with adding neutron pairs these predominantly couple to spin 0, leaving the hole in the $\nu d_{5/2}$ orbit, and this applies all the way up to $N = 64$. This is why in the calculations of magnetic moments presented in Table V the $(\nu d_{5/2})^{-1}$ configuration has always been used. The $7/2^+$ state related to a filled $\nu d_{5/2}$ orbit and an odd number of neutrons in the $\nu g_{7/2}$ orbit is in almost all isotopes found as an excited state at excitation energies ranging from 188 to 416 keV, except for ^{111}Sn, where it is the ground state. It is not understood why this predominant coupling of neutron pairs in the $\nu g_{7/2}$ orbit occurs. However, the configuration is complex, as can be seen from the g factors of the odd-neutron states in this mass region which are found to have values of about −0.30 (see column 5 in Table V), which in absolute value is considerably smaller than the modified Schmidt value of −0.576 for the $\nu d_{5/2}$ orbit (the modified Schmidt g factor for the $\nu g_{7/2}$ orbit is +0.242). Note that this issue is to some extent also related to the current debate about the ground state of ^{101}Sn being $\nu d_{5/2}$ or $\nu g_{7/2}$ (e.g., [52,53]).

As can be seen in Table V, for the heavier neutron-deficient isotopes ^{106}Ag, ^{108}Ag, and ^{110}Ag (with a 1^+ ground state and a 6^+ isomeric state), the magnetic moment for the isomeric state can be very well explained by a parallel coupled $(\pi g_{9/2})^{-3}_{7/2^+}(\nu d_{5/2})^{-1}_{5/2^+}$ configuration. The values calculated with the additivity relation [Eq. (21)] using Schmidt single particle moments or modified single particle moments are systematically lower than the experimental values, but the values calculated with experimental g factors are always very close to the experimental results.

For the 1^+ ground state of ^{106,108,110}Ag, coming from the antiparallel coupling of the $(\pi g_{9/2})^{-3}_{7/2^+}$ proton group and the $(\nu d_{5/2})^{-1}_{5/2^+}$ neutron state, the additivity rule with experimental g factors of neighboring isotopes yields values that are systematically about 0.3 to 0.5 μ_N too large. Because the correction on this 1^+ state owing to core excitations is less than 0.1 μ_N [50], this deviation is probably attributable to the mixing of other states in the wave function. The $(\pi g_{9/2})^{-3}_{7/2^+}$ proton configuration is thus firmly established for $^{106-110}$Ag.

For the lower-mass ^{102,104}Ag isotopes, Ames *et al.* [3] already pointed out that the wave function would consist

TABLE V. Magnetic moments of the even-A Ag isotopes. Experimental magnetic moments are compared with values obtained with the addition theorem [Eq. (21)] using Schmidt values, $\mu_{\rm add}^{\rm Sch}$, modified Schmidt values, $\mu_{\rm add}^{\rm mod}$, or experimental moment values from neighboring isotopes, $\mu_{\rm add}^{\rm exp}$. Note that in fact the $(\nu d_{5/2})^{-1}$ neutron configuration was used to calculate $\mu_{\rm add}^{\rm Sch}$ and $\mu_{\rm add}^{\rm mod}$ (see text). Because $g_{n,\rm exp}$ was obtained from neighboring isotopes with $I^\pi = 5/2^+$, the values for $\mu_{\rm add}^{\rm exp}$ in column 8 take into account the fact that the effective neutron configuration is a mixture of $\nu d_{5/2}$ and $\nu g_{7/2}$ coupling to a spin $5/2^+$. Further, because the Schmidt g factors for $\nu d_{5/2}$ and $\nu g_{7/2}$ are -0.765 and 0.425, respectively, the fact that $g_{n,\rm exp}$ varies between -0.252 and -0.331 (see column 5) indicates that a considerable amount of mixing between the $\nu d_{5/2}$ and $\nu g_{7/2}$ states is present. (Table adapted from Ref. [5].)

A	I^π	Configuration	$g_{p,\rm exp}$	$g_{n,\rm exp}$	$\mu_{\rm add}^{\rm Sch}$ ($\mu_{\rm N}$)	$\mu_{\rm add}^{\rm mod}$ ($\mu_{\rm N}$)	$\mu_{\rm add}^{\rm exp}$ ($\mu_{\rm N}$)	$\mu_{\rm exp}$ ($\mu_{\rm N}$)	Ref. ($\mu_{\rm exp}$)	Mix. ampl. α or β [Eq. (23)]
102	2^+	$[(\pi g_{9/2})_{7/2^+}^{-3}(\nu d_{5/2}\nu g_{7/2})_{5/2^+}]_{2^+}$	1.250(2)[a]	$-0.279(29)$[b]	3.40	3.16	2.76(1)	4.12(25)	[4]	0.66(11)
		$[(\pi g_{9/2})_{9/2^+}^{-3}(\nu d_{5/2}\nu g_{7/2})_{5/2^+}]_{2^+}$			6.81	6.14	5.05(5)			0.75(9)
	5^+	$[(\pi g_{9/2})_{7/2^+}^{-3}(\nu d_{5/2}\nu g_{7/2})_{5/2^+}]_{5^+}$			3.19	3.25	3.32(6)	4.55(65)	[42]	0.0(3)
		$[(\pi g_{9/2})_{9/2^+}^{-3}(\nu d_{5/2}\nu g_{7/2})_{5/2^+}]_{5^+}$			4.90	4.74	4.47(3)			1.0(3)
104	2^+	$[(\pi g_{9/2})_{7/2^+}^{-3}(\nu d_{5/2}\nu g_{7/2})_{5/2^+}]_{2^+}$	1.266(1)[c]	$-0.294(4)$[d]	3.40	3.16	2.792(2)	3.691(3)[e]	This work	0.79(1)
		$[(\pi g_{9/2})_{9/2^+}^{-3}(\nu d_{5/2}\nu g_{7/2})_{5/2^+}]_{2^+}$			6.81	6.14	5.129(5)			0.61(2)
	5^+	$[(\pi g_{9/2})_{7/2^+}^{-3}(\nu d_{5/2}\nu g_{7/2})_{5/2^+}]_{5^+}$			3.19	3.25	3.356(8)	3.919(3)[f]	[2]	0.72(2)
		$[(\pi g_{9/2})_{9/2^+}^{-3}(\nu d_{5/2}\nu g_{7/2})_{5/2^+}]_{5^+}$			4.90	4.74	4.525(6)			0.69(2)
106	1^+	$[(\pi g_{9/2})_{7/2^+}^{-3}(\nu d_{5/2}\nu g_{7/2})_{5/2^+}]_{1^+}$	1.261(4)[g]	$-0.252(6)$[h]	4.35	3.90	3.15(2)	2.83(20)	[4]	–
	6^+	$[(\pi g_{9/2})_{7/2^+}^{-3}(\nu d_{5/2}\nu g_{7/2})_{5/2^+}]_{6^+}$			3.38	3.50	3.79(2)	3.705(4)[i]	[40]	–
108	1^+	$[(\pi g_{9/2})_{7/2^+}^{-3}(\nu d_{5/2}\nu g_{7/2})_{5/2^+}]_{1^+}$	1.257(2)[j]	$-0.3311384(6)$[k]	4.35	3.90	3.242(5)	2.6884(7)	[43]	–
	6^+	$[(\pi g_{9/2})_{7/2^+}^{-3}(\nu d_{5/2}\nu g_{7/2})_{5/2^+}]_{6^+}$			3.37	3.50	3.572(7)	3.577(20)	[36]	–
110	1^+	$[(\pi g_{9/2})_{7/2^+}^{-3}(\nu d_{5/2}\nu g_{7/2})_{5/2^+}]_{1^+}$	1.257(2)[l]	$-0.306(1)$[m]	4.35	3.90	3.211(5)	2.7271(8)	[43]	–
	6^+	$[(\pi g_{9/2})_{7/2^+}^{-3}(\nu d_{5/2}\nu g_{7/2})_{5/2^+}]_{6^+}$			3.37	3.50	3.635(7)	3.609(4)[n]	[39]	–

[a]g factor of ^{101}Ag ($I^\pi = 9/2^+$) from Ref. [2].
[b]Average of the g factors of ^{99}Ru, ^{101}Pd, and ^{103}Cd.
[c]g factor of ^{103}Ag ($I^\pi = 7/2^+$) from Ref. [2].
[d]Average of the g factors of ^{101}Ru and ^{105}Cd.
[e]Other determinations of this magnetic moment have yielded $+3.7(2)\mu_{\rm N}$ [3] and 3.7(1) $\mu_{\rm N}$ (this work, RILIS measurement).
[f]Other determinations of this magnetic moment have yielded 3.916(8) $\mu_{\rm N}$ [1] (see also Table IV), and $+4.0(2)\mu_{\rm N}$ [3].
[g]g factor of ^{105}Ag^m ($I^\pi = 7/2^+$) from Ref. [2].
[h]Average of the g factors of ^{105}Pd and ^{107}Cd.
[i]Other determinations of this magnetic moment have yielded 3.709(4) $\mu_{\rm N}$ [25], 3.71(15) $\mu_{\rm N}$ [44], and 3.82(8) $\mu_{\rm N}$ [45].
[j]g factor of ^{107}Ag^m ($I^\pi = 7/2^+$) from Ref. [26].
[k]g factor of ^{109}Cd from Ref. [47].
[l]g factor of ^{109}Ag^m ($I^\pi = 7/2^+$) from Ref. [26].
[m]g factor of ^{111}Cd (level at 245 keV) from Ref. [48].
[n]Another determination of this magnetic moment has yielded 3.607(4) $\mu_{\rm N}$ [38].

of a $(\nu d_{5/2})_{5/2^+}^{-1}$ neutron configuration coupled to a mixed $(\pi g_{9/2})_{9/2^+}^{-3}(\pi g_{9/2})_{7/2^+}^{-3}$ proton configuration. The experimental magnetic moments of both the ground and the isomeric state in ^{104}Ag are in between the values calculated for the two pure proton-neutron configurations (see Table V) and support this suggestion. The magnetic moment of ^{104}Ag^g ($I^\pi = 5^+$) was previously determined with high precision in two independent experiments [1,2]. The measurement reported here provides a precise value for ^{104}Ag^m ($I^\pi = 2^+$) as well. This permits a more detailed analysis of the configuration mixture in the $2^+, 5^+$ doublet of states (only 6.9 keV apart) in ^{104}Ag. Writing the wave functions for both states as (see [50])

$$\psi(^{104}{\rm Ag}^{g,m}) = \alpha\big[(\pi g_{9/2})_{7/2^+}^{-3}(\nu d_{5/2})_{5/2^+}^{-1}\big]$$
$$+ \beta\big[(\pi g_{9/2})_{9/2^+}^{-3}(\nu d_{5/2})_{5/2^+}^{-1}\big], \qquad (22)$$

with α and $\beta = \sqrt{1-\alpha^2}$ the mixing amplitudes, the expectation value of the magnetic moment operator becomes

$$\langle\mu\rangle = \alpha^2\big\langle\mu\big[(\pi g_{9/2})_{7/2^+}^{-3}(\nu d_{5/2})_{5/2^+}^{-1}\big]\big\rangle$$
$$+ \beta^2\big\langle\mu\big[(\pi g_{9/2})_{9/2^+}^{-3}\nu(d_{5/2})_{5/2^+}^{-1}\big]\big\rangle. \qquad (23)$$

The mixing amplitudes, as obtained from the experimental magnetic moments, are listed in the last column of Table V and indicate a complete mixing of the two configurations (i.e., $\alpha \approx \beta \approx 1/\sqrt{2} = 0.71$) in ^{104}Ag^g ($I^\pi = 5^+$) and almost complete mixing in ^{104}Ag^m ($I^\pi = 2^+$). Performing the same analysis also for the doublet of 2^+ and 5^+ states of ^{102}Ag^m and ^{102}Ag^g, respectively (which differ only 9.3 keV in energy), indicates also almost complete mixing of the two different proton-neutron configurations in ^{102}Ag^m ($I^\pi = 2^+$), although the error bars still allow for a smaller contribution from the $(\pi g_{9/2})_{7/2^+}^{-3}$ proton configuration. As for ^{102}Ag^g ($I^\pi = 5^+$),

the experimental magnetic moment value suggests an almost pure $(\pi g_{9/2})^{-3}_{9/2^+}$ configuration, although the large error bar still allows for a sizable mixing from the $(\pi g_{9/2})^{-3}_{7/2^+}$ configuration (see Table V). A larger contribution of the $(\pi g_{9/2})^{-3}_{9/2^+}$ configuration in ^{102}Ag^g, as is apparently observed, would be in line with the fact that the ground state in ^{101}Ag has $I^\pi = 9/2^+$ and also with the magnetic moment of ^{101}Ag. Indeed, the experimental magnetic moment of ^{101}Ag, that is, $\mu = 5.627(11)\mu_N$ [2], is very close to the value of 5.67 μ_N that was calculated in Ref. [54] for the lowest $9/2^+$ state in the odd Ag isotopes based on a configuration that is dominated by the $(\pi g_{9/2})^{-3}_{9/2^+}$ proton group. New and precise measurements of the magnetic moments of the ground and isomeric states of ^{102}Ag, as well as of the lower-mass even-A Ag isotopes could help to further clarify this. An interesting new method

in this respect, viz. in-gas-cell laser spectroscopy [55], was recently reported. This method is currently being applied to the isotopes $^{97-102}$Ag [56].

[1] D. Vandeplassche, E. van Walle, J. Wouters, N. Severijns, and L. Vanneste, Phys. Rev. Lett. **57**, 2641 (1986).

[2] U. Dinger, J. Ebers, G. Huber, R. Menges, R. Kirchner, O. Klepper, T. Kühl, and D. Marx, Nucl. Phys. A **503**, 331 (1989).

[3] O. Ames, A. M. Bernstein, M. H. Brennan, and D. R. Hamilton, Phys. Rev. **123**, 1793 (1961).

[4] B. Greenebaum and E. A. Phillips, Phys. Rev. C **9**, 2028 (1974).

[5] E. van Walle, Ph.D. thesis, Kath. Universiteit Leuven, 1985, unpublished.

[6] P. Raghavan, At. Data Nucl. Data Tables **42**, 189 (1989).

[7] N. J. Stone, At. Data Nucl. Data Tables **90**, 75 (2005).

[8] H. Postma and N. J. Stone (editors), *Low-Temperature Nuclear Orientation* (Elsevier, Amsterdam, 1986).

[9] V. V. Golovko, Ph.D. thesis, University of Leuven, 2005 [http://hdl.handle.net/1979/43].

[10] E. Kugler, D. Fiander, B. Johnson, H. Haas, A. Przewloka, H. L. Ravn, D. J. Simon, and K. Zimmer, Nucl. Instrum. Methods **70**, 41 (1992).

[11] E. Kugler, Hyperfine Interact. **129**, 23 (2000).

[12] U. Köster (ISOLDE Collaboration), Radiochim. Acta **89**, 749 (2001).

[13] K. Schlösser *et al.* (ISOLDE Collaboration and NICOLE Collaboration), Hyperfine Interact. **43**, 139 (1988).

[14] J. Wouters, N. Severijns, J. Vanhaverbeke, W. Vanderpoorten, and L. Vanneste, Hyperfine Interact. **59**, 59 (1990).

[15] P. Schuurmans, Ph.D. thesis, Kath. Universiteit Leuven, 1996 (unpublished).

[16] J. Blachot, Nucl. Data Sheets **108**, 2035 (2007).

[17] V. V. Golovko *et al.*, Phys. Rev. C **70**, 014312 (2004).

[18] V. V. Golovko *et al.*, Phys. Rev. C **72**, 064316 (2005).

[19] D. Vénos, A. Van Assche-Van Geert, N. Severijns, D. Srnka, and D. Zákoucký, Nucl. Instrum. Methods A **454**, 403 (2000).

[20] D. Zákoucký, D. Srnka, D. Vénos, V. V. Golovko, I. S. Kraev, T. Phalet, P. Schuurmans, N. Severijns, B. Vereecke, and S. Versyck (NICOLE/ISOLDE Collaboration), Nucl. Instrum. Methods A **520**, 80 (2004).

[21] H. Marshak in Ref. [8], p. 769.

[22] I. S. Kraev *et al.*, Nucl. Instrum. Methods A **555**, 420 (2005).

[23] K. S. Krane, in Ref. [8], p. 31.

[24] S. Chikazumi, *Physics of Magnetism* (Wiley, New York, 1964).

[25] R. Eder, E. Hagn, and E. Zech, Phys. Rev. C **30**, 676 (1984).

[26] R. Eder, E. Hagn, and E. Zech, Phys. Rev. C **31**, 190 (1985).

[27] E. W. Duczynski, Ph.D. thesis, Universität Hamburg, 1983 (unpublished).

[28] E. Klein, in Ref. [8], p. 579.

[29] T. L. Shaw and N. J. Stone, At. Data Nucl. Data Tables **42**, 339 (1989).

[30] D. Vénos, D. Zákoucký, and N. Severijns, At. Data Nucl. Data Tables **83**, 1 (2003).

[31] R. Guin, S. K. Saha, S. M. Sahakundu, and S. Prakash, J. Radiol. Nucl. Chem. **141**, 185 (1990).

[32] F. James and M. Roos, Comput. Phys. Commun. **10**, 343 (1975).

[33] V. N. Fedosseev *et al.*, Nucl. Instrum. Methods B **204**, 353 (2004).

[34] R. A. Fox, P. D. Johnston, and N. J. Stone, Phys. Lett. A **34**, 211 (1971).

[35] H. D. Rüter, E. W. Duczynski, G. Scholtyssek, S. Kampf, E. Gerdau, and K. Freitag, in *Book of Abstracts of Invited and Contributed Papers of the Sixth International Conference on Hyperfine Interactions, Groningen, The Netherlands*, edited by L. Niesen, H. Pleiter, and H. De Waard, 1983, p. RP 8, and cited in Ref. [25].

[36] W. Fischer, H. Hühnermann, and Th. Meier, Z. Phys. A **274**, 79 (1975).

[37] F. D. Feiock and W. R. Johnson, Phys. Rev. **187**, 39 (1969).

[38] S. G. Schmelling, V. J. Ehlers, and H. A. Shugart, Phys. Rev. **154**, 1142 (1967).

[39] W. D. Hutchison, N. Yazidjoglou, and D. H. Chaplin, Hyperfine Interact. **73**, 247 (1992).

[40] S. Ohya, H. Sato, T. Izumikawa, J. Goto, S. Muto, and K. Nishimura, Phys. Rev. C **63**, 044314 (2001).

[41] S. Ohya, Y. Izubuchi, J. Goto, T. Ohtsubo, S. Muto, and K. Nishimura, Hyperfine Interact. **133**, 105 (2001).

[42] D. Vandeplassche, E. van Walle, J. Wouters, N. Severijns, and L. Vanneste, Hyperfine Interact. **22**, 483 (1985).

[43] A. Winnacker, H. Ackermann, D. Dubbers, M. Grupp, P. Heitjans, and H.-J. Stöckmann, Nucl. Phys. A **261**, 261 (1976).

[44] R. Haroutunian, G. Marest, and I. Berkes, Phys. Rev. C **14**, 2016 (1976).

[45] I. Berkes, B. Hlimi, G. Marest, E. H. Sayouty, R. Coussement, F. Hardeman, P. Put, and G. Scheveneels, Phys. Rev. C **30**, 2026 (1984).

[46] R. J. Barlow, *A Guide to the Use of Statistical Methods in the Physical Sciences* (Wiley, New York, 1989).

[47] P. W. Spence and M. N. McDermott, Phys. Lett. A **42**, 273 (1972).

[48] H. Bertschat, H. Haas, F. Pleiter, E. Recknagel, E. Schlodder, and B. Spellmeyer, Z. Phys. **270**, 203 (1974).

[49] M. H. Brennan and A. M. Bernstein, Phys. Rev. **120**, 927 (1960).

[50] H. Noya, A. Arima, and H. Horie, Suppl. Prog. Theor. Phys. **8**, 33 (1958).

[51] K. Kumar, Phys. Scr. **11**, 179 (1975).

[52] O. Kavatsyuk *et al.*, Eur. Phys. J. A **31**, 319 (2007).

[53] D. Seweryniak *et al.*, Acta Phys. Pol. B **40**, 621 (2009).

[54] V. Paar, Nucl. Phys. A **211**, 29 (1973).

[55] T. E. Cocolios *et al.*, Phys. Rev. Lett. **103**, 102501 (2009).

[56] I. Darby *et al.* (unpublished).